Photosensitizer dosimetry controlled PDT treatment planning reduces inter-individual variability in response to PDT

Xiaodong Zhou[a], Brian W. Pogue[a,d], Bin Chen[a,b], Eugene Demidenko[c], Rohan Joshi[a], Jack Hoopes[b] and Tayyaba Hasan[d]

[a]Thayer School of Engineering, Dartmouth College, Hanover, NH 03755, U.S.;
[b]Department of Surgery, Dartmouth Medical School, Hanover, NH 03755, U.S.;
[c]Section of Biostatistics and Epidemiology, Dartmouth Medical School, Hanover, NH 03755, U.S.;
[d]Wellman Center for Photomedicine, Massachusetts General Hospital, Department od Dermatology, Harvard Medical School, Boston, MA 02114, U.S.

ABSTRACT

Effective Photodynamic therapy (PDT) treatment depends on the amount of active photosensitizer and the delivered light in the targeting tissue. For the same PDT treatment protocol, variation in photosensitizer uptake between animals induces variation in the treatment response between animals. This variation can be compensated via control of delivered light dose through photodynamic dose escalation based on online dosimetry of photosensitizer in the animal. The subcutaneous MAT-LyLu Dunning prostate tumor model was used in this study. Photosensitizer BPD-MA uptake was quantified by multiple fluorescence micro-probe measurements at 3 hours after verteporfin administration. PDT irradiation was carried out after photosensitizer uptake measurement with a total light dose of 75 J/cm^2 and a light dose rate of 50 mW/cm^2. Therapeutic response of PDT treatments was evaluated by the tumor regrowth assay. Verteporfin uptake varied considerably among tumors (inter-tumor variation 56% standard deviation) and within a tumor (largest intra-tumor variation 64%). An inverse correlation was found between mean photosensitizer intensity and PDT treatment effectiveness ($R^2 = 37.3\%$, $p < 0.005$). In order to compensate individual PDT treatments, photodynamic doses were calculated on an individual animal basis, by matching the light delivered to provide an equal photosensitizer dose multiplied by light dose. This was completed for the lower-quartile, mean and upper-quartile of the photosensitizer distribution. The coefficient of variance in the surviving fraction decreased from 24.9% in non-compensated PDT (NC-PDT) treatments to 16.0%, 14.0% and 15.9% in groups compensated to the lower-quartile (CL-PDT), the median (CM-PDT) and the upper-quartile (CU-PDT), respectively. In terms of treatment efficacy, the CL-PDT group was significantly less effective compared with NC-PDT, CM-PDT and CU-PDT treatments ($p < 0.005$). No significant difference in effectiveness was observed between NC-PDT, CM-PDT and CU-PDT. The results indicate that by measuring the mean photosensitizer concentration prior to light treatment, and then adjusting the light dose appropriately, a more uniform treatment can be applied to different animals thereby reducing the inter-individual variation in the treatment outcome.

Keywords: Photodynamic therapy, photodynamic dose, photosensitizer dosimetry, heterogeneity

1. INTRODUCTION

The emerging cancer treatment modality, photodynamic therapy (PDT), has recently been accepted for the treatment of certain malignant and non-malignant diseases.[1–6] PDT involves photosensitizer (PS) localization and light irradiation to the target tissues. Upon irradiation, PS molecules are excited, which interact with surrounding molecules, leading to the generation of singlet oxygen and/or free radicals that are toxic to cells.[5, 7–10] The massive production of singlet oxygen is thought to be the major mechanism behind tumor cell lysis. Over

Further author information: (Send correspondence to X.Z.)
X.Z.: E-mail: Xiaodong.Zhou@Dartmouth.edu, Telephone: 1 603 646 2859
B.W.P.: E-mail: Pogue@Dartmouth.edu, Telephone: 1 603 646 3861

the past 30 years, PDT protocols have been developed for numerous types of cancers and pre-cancers conditions. FDA approved PDT sites include skin, head and neck and gastrointestinal tract.[11–13] To date, most clinical PDT treatments have been performed using a predetermined PS dose, a fixed time interval between photosensitizer and light administration, and a stipulated irradiation time with a fixed incident light irradiance (in units of mW/cm^2 for surfaces, or specified as mW/cm for cylindrical illuminators). Using this protocol, most pre-clinical and clinical PDT studies indicate a considerable variation in the treatment response.[12] Although some of this treatment response variation can be due to the biologic variation in response to therapy for different histologic subtypes or different tumor geometries, the issue of varying photosensitizer concentration in the tumor tissue is definitely a contributing factor. As a matter of fact, significant heterogeneity in PS tumor uptake has been demonstrated in both preclinical and clinical PDT studies.[14, 15] Yet this issue is also the one that can be readily addressed with *in vivo* dosimetry measurements, by simply adding more light dose where there is lower drug dose. There is a well known reciprocity between drug and light dose, which has been demonstrated in experimental tumors for several years.[16–19] Recent developments of fluorescence detection techniques have made online dosimetry of PS possible. Both fiber based dosimeters[20] and wide-field fluorescence imaging dosimeters[21–24] have been designed and tested in phantom, animal and clinical studies. These fluorescence measurements can provide information about photosensitizer concentration in different tumors and in different areas within a tumor. Currently, most PS dosimetry systems focus on the overall change of PS concentration without enough attention on the variation of measurements within each subject. This is partially because some PS dosimetry systems tend to sample large tissue volumes and therefore are not able to detect PS uptake heterogeneity. The micro-sampling probe in the dosimeter system used in this study allows detection of PS variation in tumor tissue on the size scale of 100 microns. It is generally accepted that photodynamic therapy dose is defined as the number of photons absorbed by photosensitizer per unit volume of tissue.[25, 26] This determination is readily calculated by multiplying the concentration of PS by its extinction coefficient and the light fluence incident in that location. Thus, in order to deliver the same PDT dose, as the concentration of PS changes the light fluence should be adjusted accordingly to compensate for this PS inter-subject variation. The objective of this study is to examine the feasibility and outcome of individual PDT regimen based on PS dosimetry measurements in a well-characterized rat prostate tumor model., The PS tumor uptake variation was assessed using a micro-sampling PS dosimetry system and, based on these measurements, the light dose was adjusted to determine whether such a modification would improve treatment outcome. If this overall hypothesis is true, it would open up the possibility of subject-customized PDT dosimetry along the lines of radiation therapy treatment planning.

2. MATERIALS AND METHODS

2.1. Animals and tumor model

Male Copenhagen rats with an average body weight of 120 g-150 g, were used for this study (Charles River Laboratories, Wilmington, MA). All animals were housed in the Dartmouth Medical School animal facility. This facility and program are AAACAC accredited and adhere to all USDA guidelines for animal research use. The animals were housed in a temperature controlled environment with a 12-hr light/dark cycles, having free access to water and standard laboratory diet. All procedures and experiments were approved by the Dartmouth College Institutional Animal Care and Use Committee. The animals were anesthetized using an intra-muscular injection of a mixture of Ketamine and Xylazine at a dose of 90 mg/Kg and 10 mg/Kg respectively. A subcutaneous tumor was introduced by injection of 1×10^5 cells of the Dunning prostate tumor R3327 MAT-LyLu (Metastatic AT-Lymph Node and Lung),[27] on the right flank in a volume of 50 μl. Animals were followed daily to track the tumor growth. Tumors were treated when they reach 150-300 mm^3 (approximately 7 days post injection).

2.2. Photosensitizer

A liposomal formulation of the photosensitizer benzoporphyrin derivative (BPD),[28, 29] verteporfin-for-injection (QLT Inc., Vancouver, BC, Canada), was used for all studies. Following reconstitution, animals received 1.0 mg/Kg BPD intravenously (tail vein). Photosensitizer dosimetry was then performed, and tumors were irradiated 3 hours after PS administration.

2.3. Photosensitizer dosimetry

Immediately prior to light treatment, the skin over the tumor area was carefully removed for measurement of the PS fluorescence in the tissue. The surrounding vasculature was preserved as much as possible to minimize bleeding and changes in optical properties of the tumor. PS concentration measurement was achieved using a customized commercial fluorimeter system (Aurora Optics, Inc., Hanover, New Hampshire) at 20 distinct locations, sampling 5 times at each site. The set of 100 data points for each animal were used to analyze the intra-tumor variation of fluorescence intensities for each animal. The average of 100 data points for each animal was used to represent the PS uptake by the individual animal and for the analysis of inter-tumor variation. All the measurements were recorded 3 hours after PS administration. The fluorimeter system employed a 405 nm diode laser, a 660 nm long-pass filter and a photomultiplier tube for detection. The fiber bundle contained 6 detection fibers and a center excitation fiber. The six detection fibers each has 100 micron diameter in order to constrain the distance of tissue sampled to be smaller than the average scattering distance (mean free path) of tissue, which is typically 100-200 microns. The sampling time for each measurement was limited within 0.5 seconds, so that less than 10% photobleaching occurred when a repeated sampling was taken from an individual spot on the tissue.[30–32]

2.4. Photodynamic dose calculation and Photodynamic therapy treatments

Irradiation of tumors was achieved using a 1 Watt maximum, 690 nm wavelength diode laser (Applied Optronics, CT) delivered via a 140 μm diameter optical fiber. Laser beam was collimated through a coupling lens on the end of the fiber to a 1cm diameter beam spot over the tumor surface. The tumors received an average incident irradiance 50 mW/cm^2, as evaluated by an optical power meter (Thorlabs Inc, NJ). The time of irradiation was fixed for the first two groups, and then varied in the latter three groups to maintain a group where each animal received a fixed total dose, as defined below. Tumor-bearing animals were divided into five groups of 11-20 animals. The control group and standard PDT group were as follows: (a) PS-only Control group (CTRL): 20 animals were injected verteporfin intravenously and received PS dosimetry without laser illumination 3 hours post injection. (b) Non-Compensated PDT treatment group (NC-PDT): 20 animals received the i.v. injection of Verteporfin-For-Injection, and photosensitizer dosimetry 3 hours post injection. Animals received the PDT irradiation right after PS dosimetry with total light dose of 75 J/cm^2 and an average light irradiance of 50 mW/cm^2. Photodynamic dose was estimated by multiplying the photosensitizer uptake of each individual and the total light dose of 75 J/cm^2. The effect of compensating the light dose to the photosensitizer concentration was examined in three ways. Since the fluorescence from each animal was measured in up to 100 samples, each subject had a distribution of values from which to estimate the photosensitizer dose *in vivo*. It was hypothesized that compensating the light dose of each animal to achieve a total PDT dose equivalent to that calculated by the mean PS dose multiplied by 75 J/cm^2 might be optimal. However, alternative measures of the photosensitizer dose based upon the histogram of values from each animal, would be to use the lower quartile of the distribution, or possibly the upper quartile of the distribution. In order to test if the mean lower quartile, or mean upper quartile values of the PDT dose were better suited to reduce variance in treatment effect, treatment groups were included which received PDT doses equivalent to the lowest photosensitizer quartile and the highest photosensitizer quartile, each multiplied by the light fluence of 75 J/cm^2. This was achieved by each animal being given a light dose which was compensated to achieve the same total PDT dose (light dose multiplied by drug dose). These formulas used the following definitions below. In these definitions, the photosensitizer concentration distribution in the entire control group was used to calculate the mean, $[PS]_C$, the mean of the upper quartile $[PS_{UQ}]_C$ and the mean of the lower quartile $[PS_{LQ}]_C$. In the same way, for each individual animal in the compensated groups they were used to calculated the mean photosensitizer concentration, $[PS]_i$, or the lower quartile $[PS_{LQ}]_i$, or the upper quartile $[PS_{UQ}]_i$. Once calculated for each animal, the compensated dose was estimated and the animals were treated in one of the three groups according to the formulas:

(c) Compensation-to-Median PS value treatment group (CM-PDT): 17 animals. Total light dose for each subject was calculated from the dose calculation formula:

Total light dose = $(75 J/cm^2) \times ([PS]_C)/([PS]_i)$

(d) Compensation-to-Lower PS quartile PDT treatment group (CL-PDT): 11 animals received photosensitizer dosimetry 3 hours after verteporfin injection. The total light dose for each subject was estimated from the formula:

Total light dose $= (75 J/cm^2) \times ([PS_{LQ}]_C)/([PS_{LQ}]_i)$

(e) Compensation-to-Upper PS quartile, PDT treatment group (CU-PDT): 19 animals. The total light dose for each subject was calculated from the formula:

Total light dose $= (75 J/cm^2) \times ([PS_{UQ}]_C)/([PS_{UQ}]_i)$

2.5. Tumor Regrowth Assay and Model Based Interpretation

Tumor regrowth assay was used to quantify the treatment effects of photodynamic therapy. Width (a), length (b) and height (c) were measured with slide calipers to determine the tumor volume, and calculations were performed using the formula $V = \frac{\pi}{6} \times a \times b \times c$. The longitudinal tumor volume data, as a function of time (in days) after treatment, are displayed on a semi-logarithmic scale. The advantage of the semi-logarithmic versus regular scale is that exponentially growing tumors follow a straight line so that the effects of the tumor growth delay are clearly seen. Moreover, expressing observations as $v_t = ln(V_t)$, where V_t is the tumor volume at time t, facilitates modeling of tumor growth and regrowth in treatment groups and their statistical comparison.[33] The following tumor regrowth model[33] has been applied to mathematically describe the dynamics of treated tumors: $v_t = \alpha + \beta t - \ln(SF\%)\left(e^{-\delta t} - 1\right)$, where α is the log tumor volume before the treatment, β is the growth rate of unaffected tumor cells, δ is cell loss constant at which the treated cells die, and $SF\%$ is survival fraction. This model allows computing other treatment endpoints such as tumor growth delay (TGD) computed as and doubling time (DT) as the solution to the equation . Tumor growth delay (TGD), doubling time (DT) and survival fraction ($SF\%$) were used to determine variations of tumor response within and between groups.

3. RESULTS

### 3.1. Inter-tumor and intra-tumor variation in photosensitizer uptake

Photosensitizer dosimetry measurements were performed on 40 animals (20 from CTRL group, 20 from NC-PDT group) at 3 hours post injection of verteporfin. Photosensitizer fluorescence intensity measured via PS dosimeter (Aurora Optics, Lebanon, NH) varied considerably between tumors and between locations on each tumor. *Figure* 1(a) demonstrates two tumors, one with small intra-tumor variation (coefficient of variation = 11.9%) and one with a large intra-tumor variation (coefficient of variation = 64.2%)(coefficient of variation = standard deviation to mean ratio). This information illustrates how animals may have different photosensitizer uptake distributions, *e.g.* animal B has a higher percentage of low photosensitizer uptake area compared with animal A, possibly due to necrotic areas or damaged blood flow. The overall intra-tumor variation summarized from 40 animals is shown in *Figure* 1(b). Differences in data distribution for individual animal and a larger population are shown. Inter-tumor variation of photosensitizer uptake is shown in *Figure* 1(c). This graph summarizes the average photosensitizer uptake from 40 animals (coefficient of variation: 56.9%). Photosensitizer uptake is represented by the average of 100 data points measured from each tumor. In *Figure* 1(a), the mean and standard deviation are 0.291 and 0.082 for rat A (smaller variation), and 0.296 and 0.190 for rat B (larger variation), which correspond to coefficient of variation values of 11.9% and 64%, respectively. The mean and standard deviation in *Figure* 1(b) were 0.50 and 0.33, and coefficient of variation was 66.0%. In *Figure* 1(c), the mean and standard deviation values are 0.51 and 0.29, corresponding to a coefficient of variation of 57%.

### 3.2. Inter-tumor variation in treatment response

To assess the tumor response to PDT treatment, the tumor volume was measured daily immediately following PDT treatment. The animals in the photosensitizer only control group showed faster and less variable growth dynamics (*Figure* 2). The mean $\pm$ standard variation of tumor volume on day one and day six were 213 ± 71 mm^3 and 2224 ± 735 mm^3. The coefficients of variation were 33.4% and 33.1% respectively. The animals in the Non-Compensated PDT treatment group showed considerably more variation in growth dynamics after treatment. On day 1, the mean tumor volume was 204 mm^3 with a standard deviation of 55 mm^3, which corresponds to a coefficient of variation of 26.9%. On day 8, the mean tumor volume increased to 1753 ± 1151 mm^3, corresponding to coefficient of variation of 65.7%. By fitting the tumor volume to a double-exponential regrowth model, the control tumors were found to grow at an exponential rate of , with a doubling time of 1.48 days. Non-compensated PDT treated tumors showed an average growth delay of 3.54 days (standard deviation: 0.41, coefficient of
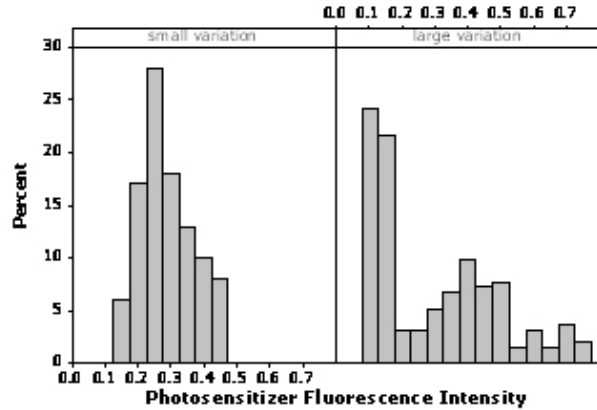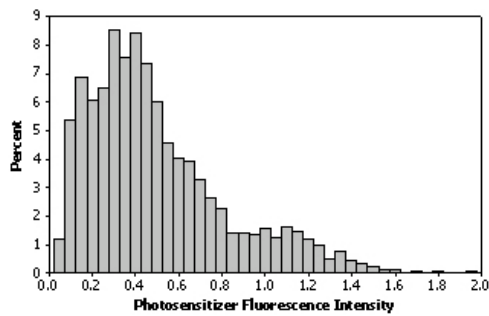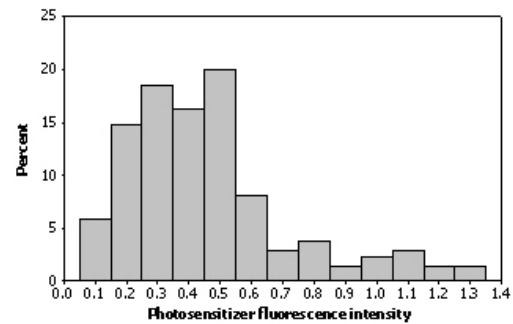
Figure 1. (a) Fluorescence intensity histogram for two individual animals. Coefficients of variation for the fluorescence intensity measurement are 11.9% and 64.2% for the left and right panel respectively. (b) Overall intra-tumor variation from 40 animals. Coefficient of variation is 66.0%. (c) Overall inter-tumor variation in photosensitizer uptake, the mean and standard deviation are 0.51 and 0.29, corresponding to a coefficient of variation of 57%.

Tx. Group	DT	TGD	SF%
NC-PDT	3.42 ± 0.41 (12.0%)	3.54 ± 0.53 (15.0%)	19.68 ± 4.94 (24.9%)
CL-PDT	2.75 ± 0.28 (10.1%)	2.22 ± 0.33 (14.9%)	35.75 ± 5.72 (16.0%)
CM-PDT	3.39 ± 0.26 (7.5%)	2.84 ± 0.28 (9.9%)	27.12 ± 3.78 (14.0%)
CU-PDT	3.72 ± 0.30 (8.1%)	3.29 ± 0.32 (9.7%)	21.77 ± 3.47 (15.9%)

Table 1. Summary of tumor doubling time, tumor growth delay and surviving fraction for all treatment groups.

variation: 15.0%), tumor doubling time 3.42±0.41 days (coefficient of variation: 12.0%) and surviving fraction of 19.7±4.9% (coefficient of variation 24.9%) See Table 1 for these details.

3.3. Correlation between BPD tumor uptake and PDT treatment outcome

Tumor response to PDT was evaluated as a function of tumor BPD uptake at the time of illumination. Survival fraction was used to represent the tumor response to PDT treatment. The survival fraction was found inversely correlated with BPD uptake as shown in *Figure* 3, (($R^2 = 37.3\%$, $p < 0.05$)).

3.4. Compensated PDT reduces the inter-tumor variation in treatment response

Compensated PDT dose calculations were based on the photosensitizer dosimetry histogram values. All measurements were performed 3 hours after intravenous verteporfin injection. Inter-tumor (macroscopic) variations
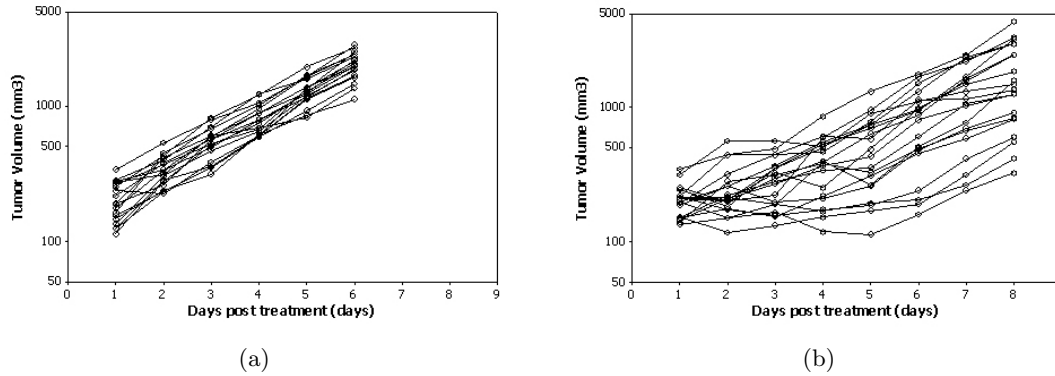
Figure 2. Tumor growth dynamics of animals in CTRL group (a) and NC-PDT group (b). Coefficients of variation for tumor volumes are 33.4% and 33.1% at day one and day six for CTRL animals, and 26.9% and 65.7% at day one and day eight for NC-PDT animals
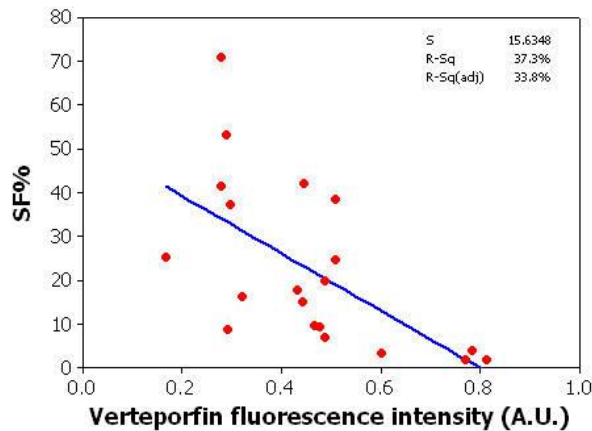

Figure 3. Correlation between BPD tumor uptake level and PDT treatment responses. 20 animals were included.

in the mean photosensitizer uptake are illustrated in *Figure* 4(b)4(d)4(f) for CU-PDT, CM-PDT and CL-PDT groups respectively. The mean and standard deviation for macroscopic photosensitizer uptake are 0.49 and 0.16 for CL-PDT (coefficient of variation = 33%), and 0.44 and 0.13 for CM-PDT (coefficient of variation = 30%) and 0.50 and 0.17 for CU-PDT (coefficient of variation = 34%). Overall intra-tumor (microscopic) variations in BPD uptake are shown in *Figure* 4(a)4(c)4(e) for three compensated PDT groups. The mean and standard deviation are 0.49 and 0.19 for CL-PDT (coefficient of variation = 39%), and 0.44 and 0.18 for CM-PDT (coefficient of variation = 41%) and 0.51 and 0.21 for CU-PDT (coefficient of variation = 41%). Compensated PDT treatments were performed 8 days following MAT-LyLu tumor implantation. The averaged volumes of the tumors being treated were 220.7±54.0 mm3 (24% variation), 220.1±46.2 mm^3 (21%), and 190.9±54.6 mm^3 (29%) for CL-PDT, CM-PDT and CU-PDT. Tumor volumes were recorded everyday after treatments (*Figure* 5(a)5(b)5(c)). Variations of tumor volume on day 8 were 35%, 31% and 42% for CL-PDT, CM-PDT and CU-PDT. These values are significantly less than the variation in tumor volume on day 8 of Non-Compensated PDT treatment group (p<0.05) (*Figure* 3.4). Coefficient of variation in doubling time (DT), tumor growth delay (TGD) and surviving fraction (SF%) were 11.1%, 14.9% 16.0% for CL-PDT, 7.5%, 9.9% and 14.0% for CM-PDT and 8.1%, 9.7% and 15.9% for CU-PDT. Variations in these characteristic parameters are significantly less than was observed in compensated PDT treatments (p<0.05).
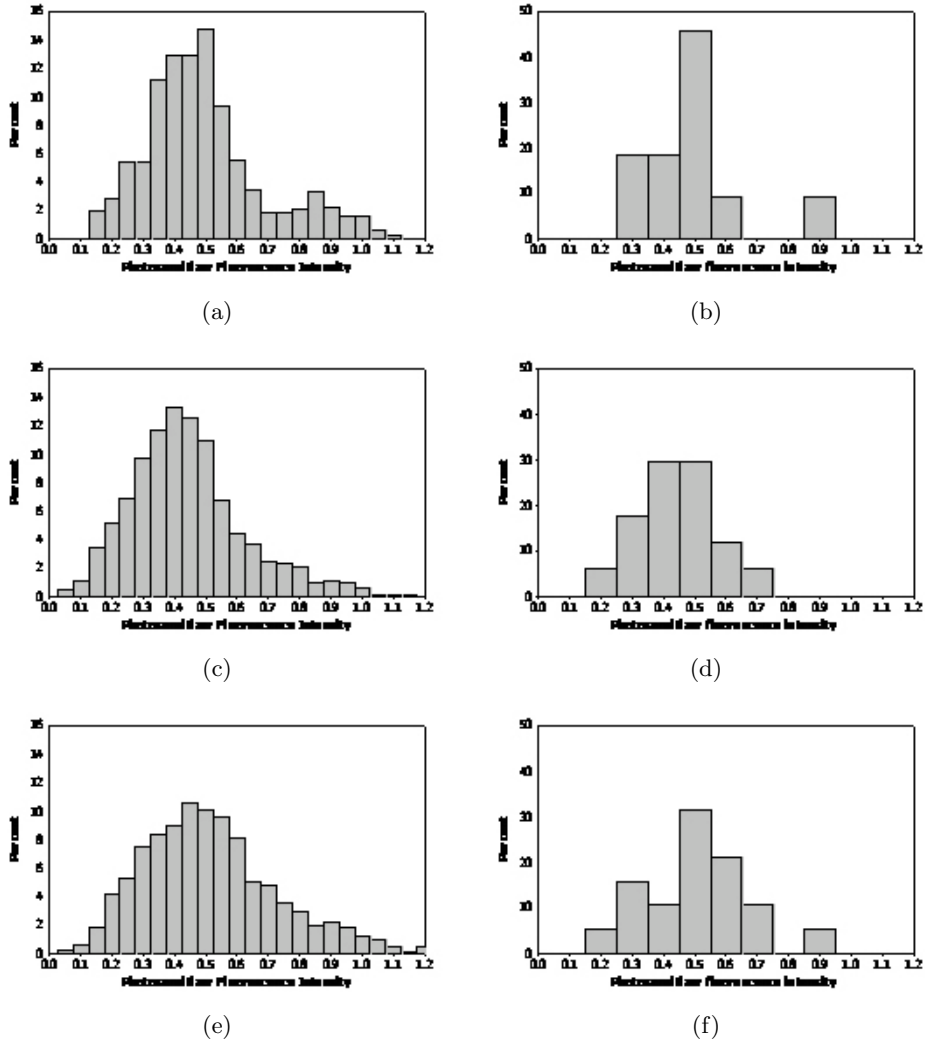
(a)

(b)

(c)

(d)

(e)

(f)

Figure 4. Distributions of intra-tumor (microscopic) variation (a, c, e) and inter-tumor (macroscopic) variation (b, d, f) in photosensitizer uptake for CU-PDT (a, b), CM-PDT (c, d) and CL-PDT (e, f) animals.
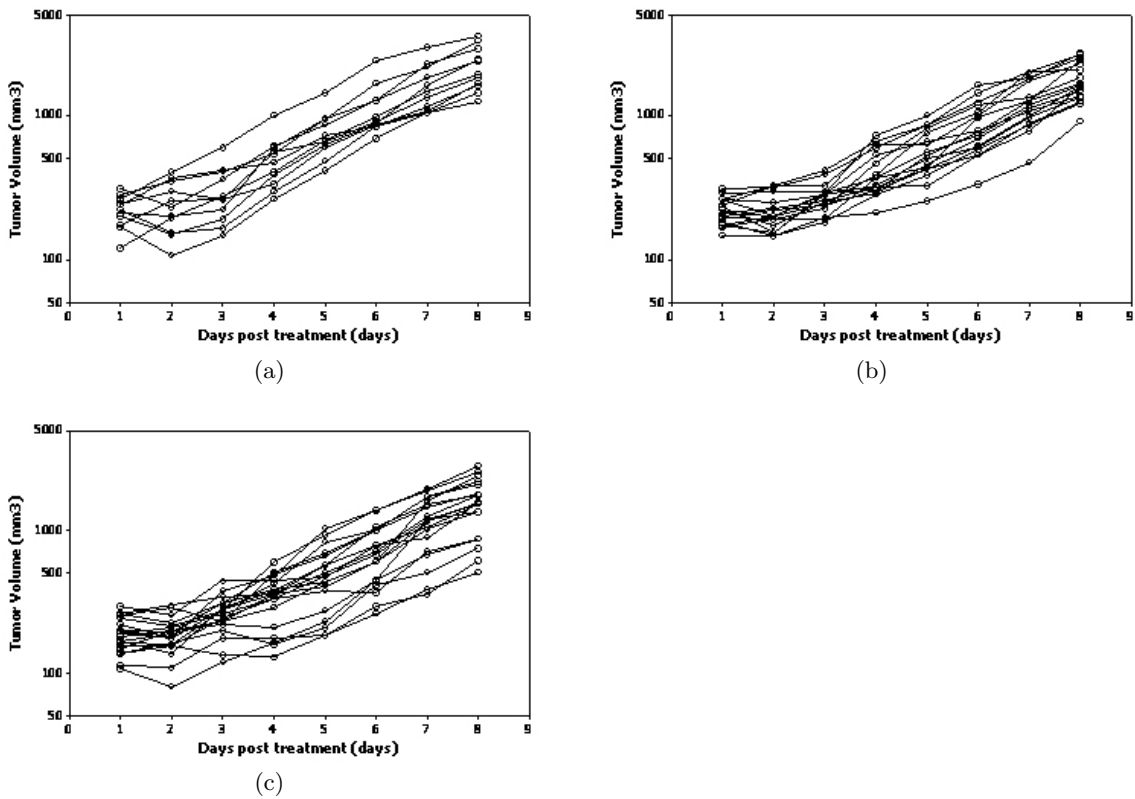
(a)

(b)

(c)

Figure 5. Tumor growth dynamics of animals in compensated PDT groups. Coefficients of variation for tumor volumes are 24% at day one and 35% at day eight for CL-PDT (a), 21% at day one and 31% at day eight for CM-PDT (b), and 29% at day one and 42% at day eight for CU-PDT (c).
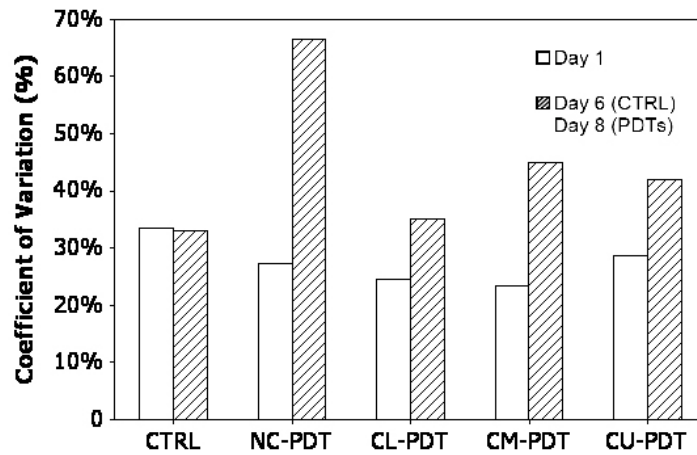

Figure 6. Coefficients of variation for tumor volumes. Data shown are CTRL group (day one and day six), and NC-PDT, CL-PDT, CM-PDT, CU-PDT groups (day one and day eight). CTRL = PS only control group; NC-PDT = Non-Compensated PDT; CL-PDT = Compensated-to-Lower PS quartile PDT treatment group; CM-PDT = Compensated-to-Median PS value PDT treatment group; CU-PDT = Compensated-to-Upper PS quartile PDT treatment group.
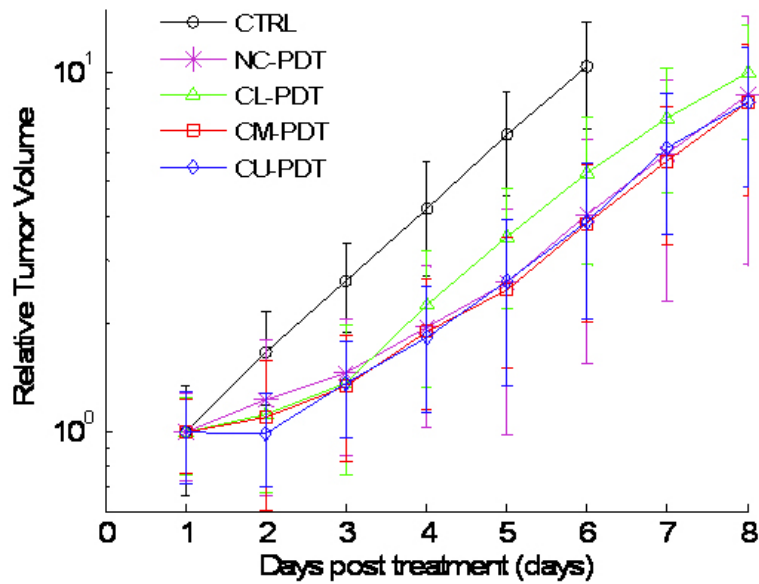
Figure 7. Averaged tumor volume on each day post treatment for all the groups. Error bars represent the standard deviation of measured tumor volumes. Open circle = CTRL; star = NC-PDT; open triangle = CL-PDT; open square = CM-PDT; open diamond = CU-PDT. Each point represents the mean ± SD.

Table 2. Paired comparisons of doubling time, tumor growth delay and surviving fraction for all treatment groups.

Tx. Group	DT	TGD	SF%
CL-PDT vs NC-PDT	0.18	0.03 *	0.03 *
CM-PDT vs NC-PDT	0.94	0.24	0.23
CU-PDT vs NC-PDT	0.56	0.69	0.73
CM-PDT vs CL-PDT	0.09	0.16	0.21
CU-PDT vs CL-PDT	0.02 *	0.02 *	0.04 *
CU-PDT vs CM-PDT	0.4	0.29	0.3

3.5. Comparison of treatment efficacy of PDT treatments

All treatments showed effective control of tumor growth, but CL-PDT had significantly less control of the tumor growth as compared with NC-PDT, CM-PDT and CU-PDT (*Figure* 3.5). Paired comparisons of doubling time, tumor growth delay and surviving fraction showed CL-PDT had significantly shorter doubling time, as well as significantly shorter tumor growth delay and larger surviving fraction (Table 1 and Table 2).

4. DISCUSSIONS

Compared with the advanced treatment planning in radiation therapy, PDT dosimetry, dose distribution calculation and treatment planning are still in their infancy. During the last twenty years, many PDT dosimetry tools have been designed and tested. These include physical parameter dosimetry, *e.g.* light dosimetry,[34, 35] PS dosimetry,[20–24, 30, 32] oxygen dosimetry,[36–40] singlet oxygen generation[41–44] and physiological parameter dosimetry, *e.g.* blood flow measurement,[45] or NADH measurement.[46] Fluorescence dosimetry has been proposed for a long time and has considerable discussion about it as perhaps the most ideal and stable way to measure dose *in vivo*, yet to this date no clinical implementation of the concept has been used to tailor individual patient dose. This study was designed to demonstrate the variation in PS uptake, the variation in tumor biological response to

PDT treatment, their correlation and do a preliminary examination of the advantage of PS-dosimetry controlled PDT treatment planning.

There is considerable variation in PS uptake between tumors and within a tumor observed in this study, with 57% coefficient of variation between animals and a factor of 14 in total variation of the mean value. After the PS is injected in the animal, PS molecules are distributed in the vasculature tree, transported across the vessel wall, and diffused in the tumor parenchyma.[47] The variation of PS concentration at different areas of tumor can be explained by the variations in these PS transport processes, *e.g.* different vasculature architecture, capillary permeability, and tumor interstitial diffusivity.[47] *Figure* 1(c) illustrates that different animals may have different PS microscopic distributions even when they have the same mean PS uptake. For animal A, the PS concentration histogram can be fitted well with a normal distribution; while for animal B, there is a higher fraction of the lowest PS measurements, which probably indicates animal B has many less well-perfused vessels. The probe used in this study is designed to sample superficial regions of tissue in order to reduce the effect of photon scattering.[20] However, this is an artifact of the measurement technique which must be interpreted appropriately as the data are examined, and is a problem which is not readily solved. Probes which sample deeper in the tumor can be developed, but have the problem of sampling larger volumes of tissue, and so do not give a good measure of the tissue heterogeneity. Thus, an underlying hypothesis to this interpretation is that the measurements from the surface of the tumor can be used to represent overall PS uptake by the tumor, if sufficient sampling spots are taken. This may not be true, but presents an attempt to acquire multiple point data sets from a solid tumor *in vivo*, and has been examined by comparison with frozen section microscopy analysis in a previous paper, showing reasonable agreement.[15] The data in *Figure* 1(b) suggests there is considerable inter-tumor variation in PS uptake (as much as 14 fold increase in some animals). This large degree of variation is of course problematic, especially for the case as used in clinical implementation where no PS dosimetry is implemented, and every subject receives the same stipulated light irradiation. Subjects with lower PS uptake could be under-treated, resulting in partial response or even no response to the PDT treatment, or potentially even worse complications such as enhanced aggressiveness of the disease.[48] The origin of PS uptake inter-tumor heterogeneity is not completely understood, however it appears to be due to the chaotic patterns of vessels within tumors which lead to a highly heterogeneous and unpredictable environment at the microscopic level.[47] It is interesting to compare the inter-tumor variation and intra-tumor variation in PS delivery. First, individual tumors have significantly different PS microscopic distributions, as shown in *Figure* 1(a); second, the PS uptake variation at different points within one tumor is not easily predicted and bears no correlation to the variation between separate tumors; third, the overall relative intra-tumor variation estimated from a large group of tumors, is greater than the inter-tumor variation from the same population, indicating again that the micro-heterogeneity of each tumor dominates the variance observed.

Using a well accepted tumor regrowth assay[49] and a double exponential model,[33] the growth characteristics were assessed for the MAT-LyLu Dunning prostate tumor model. Fitting the tumor growth dynamics to the double-exponential model for each subject indicates significant variation in the treatment response (*Figure* 2). This treatment response indicates that variation in photodynamic dose delivered to individual animals must be present. In fact, there is a significant correlation between the treatment efficacy and the BPD level in the tumor. This is not surprising, since, in this study, PDT treatments were carried out on the tumors with approximately same geometry, with similar light fluence. Thus, it appears that the variation in the delivered photons to tissue/tumor per unit time can be ignored, and the variance between animals is largely attributed to drug uptake variation.

Based on these observations, it is reasonable to assume that adjusting the irradiation time is a reasonable method for compensating for the variation in PS uptake and for keeping the photodynamic dose constant. The three target photodynamic doses studied represent lowest-quartile, median and upper quartile of the photodynamic doses in the Non-Compensated PDT group. It is not surprising to observe that the treatment efficacy of CL-PDT is significantly less than the other treatment groups, since a lower photodynamic dose is delivered to these animals. Other treatment groups did not show a treatment difference (*Figure* 3.5, Table 1 and Table 2). This indicates that increasing the irradiation time alone will result in a depletion of PS, and the tumor could be under-treated. Although the treatment efficacy are different, the variations in growth dynamics are significantly reduced for all three compensated PDT groups. However, there is still a 11-20% higher variation as compared

with the control animals (*Figure* 3.4) This could be explained by variation in tumor oxygenation and/or variation in PS photobleaching dynamics.

There are still other factors besides photosensitizer concentration which will significantly affect the tumor treatment efficacy. For example, tumor oxygenation could be monitored non-invasively, yet this is challenging.[36–39, 50–54] Even with tumor oxygenation microscopic distributions, (percentage of hypoxia, etc.), adjusting the irradiation time alone is not a practically useful option for routine treatment monitoring, at this stage of the technology development. For a tumor with higher percentage of hypoxia fraction, and lower PS uptake, increasing the light irradiation time with a stipulated irradiance would still likely be insufficient as the lack of photosensitizer and oxygen is a multiplicative effect, requiring prohibitively long irradiation times for sufficient effect and photobleaching of the PS may still take place from non-oxygen dependent mechanisms. Alternatively, different light irradiation schemes can be performed, *e.g.* decreasing the irradiance, while keep the total radiation dose same. This will also make the irradiation time longer, but will allow the oxygen and PS to re-perfuse in the tumor. Another option is to alter the tumor oxygenation itself, by the application of inflammatory mediators, *e.g.* histamine, bradykinin, substance P, or through oxygen or carbogen breathing. These agents may cause a rapid transient increase in endothelial permeability or plasma oxygenation and result in a plasma leakage.[55–61] Variation in photobleaching dynamics is another problem that needs to be solved. The observed bleaching rate can be heterogeneous, where different PS and different tumor environments can result in altered photobleaching rates. Each of these issues are complex and are themselves areas of intense research effort in PDT mechanisms. In this paper, the focus has remained on photosensitizer dosimetry, mainly because it is easily implemented, has high potential impact, and yet remains untested in clinical trials. The important observation of this study is that PS fluorescence can be a useful metric of treatment effect and can be used to correct for the total dose required for treatment on an individual subject basis. Follow up of this study will involve studying other treatment outcome metrics such as tumor cure rate, to determine if the effect holds for the conditions required for human tumor studies. For clinical and experimental work, several real-time PS dosimeters have been designed and tested for online, real-time measurement of PS concentration in the tumors. With dynamic PS concentration information, it should be possible to develop a real-time treatment planning methodology which will improve the homogeneity of treatment outcome.

5. CONCLUSIONS

There are considerable inter-tumor and intra-tumor variations in verteporfin PS concentration uptake within tumors and between tumors. The variation of PS between individual tumors leads to a variation in treatment response following PDT treatment. If a prescribed light irradiance and irradiation time is used based upon PS fluorescence dosimetry measurements, the tumors regrowth rates become less variable between subjects in the same treatment group. In the future, PS-dosimetry and treatment planning of different light radiation doses should be examined as a real option for standard treatment in PDT.

ACKNOWLEDGMENTS

REFERENCES

1. A. M. Fisher, A. L. Murphree, and C. J. Gomer, "Clinical and preclinical photodynamic therapy," *Lasers Surg Med* **17**(1), pp. 2–31, 1995.
2. C. J. Gomer, "Preclinical examination of first and second generation photosensitizers used in photodynamic therapy," *Photochem Photobiol* **54**(6), pp. 1093–107, 1991.
3. R. A. Hsi, D. I. Rosenthal, and E. Glatstein, "Photodynamic therapy in the treatment of cancer: current state of the art," *Drugs* **57**(5), pp. 725–34., 1999.
4. S. M. Keller, "Photodynamic therapy. Biology and clinical application," *Chest Surg Clin N Am* **5**(1), pp. 121–137, 1995.

5. H. I. Pass, "Photodynamic therapy in oncology: mechanisms and clinical use," *J Natl Cancer Inst* **85**(6), pp. 443–56, 1993.

6. W. M. Sharman, C. M. Allen, and J. E. van Lier, "Photodynamic therapeutics: basic principles and clinical applications," *Drug Discov Today* **4**(11), pp. 507–517, 1999.

7. D. E. Dolmans, D. Fukumura, and R. K. Jain, "Photodynamic therapy for cancer," *Nat Rev Cancer* **3**(5), pp. 380–7, 2003.

8. J. S. McCaughan, "Photodynamic therapy: a review.," *Drugs Aging* **15**, pp. 49–68, Jul 1999.

9. M. Ochsner, "Photophysical and photobiological processes in the photodynamic therapy of tumours," *J Photochem Photobiol B* **39**(1), pp. 1–18, 1997.

10. C. H. Sibata, V. C. Colussi, N. L. Oleinick, and T. J. Kinsella, "Photodynamic therapy: a new concept in medical treatment," *Braz J Med Biol Res* **33**(8), pp. 869–80, 2000.

11. J. A. Carruth, "Clinical applications of photodynamic therapy," *Int J Clin Pract* **52**(1), pp. 39–42, 1998.

12. C. Hopper, "Photodynamic therapy: a clinical reality in the treatment of cancer," *Lancet Oncol* **1**, pp. 212–9, 2000.

13. R. van Hillegersberg, W. J. Kort, and J. H. Wilson, "Current status of photodynamic therapy in oncology," *Drugs* **48**(4), pp. 510–27, 1994.

14. T. M. Busch, S. M. Hahn, E. P. Wileyto, C. J. Koch, D. L. Fraker, P. Zhang, M. Putt, K. Gleason, D. B. Shin, M. J. Emanuele, K. Jenkins, E. Glatstein, and S. M. Evans, "Hypoxia and Photofrin uptake in the intraperitoneal carcinomatosis and sarcomatosis of photodynamic therapy patients," *Clin Cancer Res* **10**(14), pp. 4630–8, 2004.

15. B. W. Pogue, B. Chen, X. Zhou, and P. J. Hoopes, "Analysis of sampling volume and tissue heterogeneity on the in vivo detection of fluorescence," *J Biomed Opt* **10**(4), p. 41206, 2005.

16. S. G. Bown, C. J. Tralau, P. D. Smith, D. Akdemir, and T. J. Wieman, "Photodynamic therapy with porphyrin and phthalocyanine sensitisation: quantitative studies in normal rat liver," *Br J Cancer* **54**(1), pp. 43–52, 1986.

17. T. J. Farrell, B. C. Wilson, M. S. Patterson, and M. C. Olivo, "Comparison of the in vivo photodynamic threshold dose for photofrin, mono- and tetrasulfonated aluminum phthalocyanine using a rat liver model," *Photochem Photobiol* **68**(3), pp. 394–9, 1998.

18. K. T. Moesta, W. R. Greco, S. O. Nurse-Finlay, J. C. Parsons, and T. S. Mang, "Lack of reciprocity in drug and light dose dependence of photodynamic therapy of pancreatic adenocarcinoma in vitro," *Cancer Res* **55**(14), pp. 3078–84, 1995.

19. M. S. Patterson, B. C. Wilson, and R. Graff, "In vivo tests of the concept of photodynamic threshold dose in normal rat liver photosensitized by aluminum chlorosulphonated phthalocyanine," *Photochem Photobiol* **51**(3), pp. 343–9, 1990.

20. B. W. Pogue and G. Burke, "Fiber-optic bundle design for quantitative fluorescence measurement from tissue," *Applied Optics* **37**(31), pp. 7429–7436, 1998.

21. R. Cubeddu, A. Pifferi, P. Taroni, A. Torricelli, G. Valentini, D. Comelli, C. D'Andrea, V. Angelini, and G. Canti, "Fluorescence imaging during photodynamic therapy of experimental tumors in mice sensitized with disulfonated aluminum phthalocyanine," *Photochem Photobiol* **72**(5), pp. 690–5, 2000.

22. A. J. Pope, A. J. MacRobert, D. Phillips, and S. G. Bown, "The detection of phthalocyanine fluorescence in normal rat bladder wall using sensitive digital imaging microscopy," *Br J Cancer* **64**(5), pp. 875–9, 1991.

23. G. A. Wagnieres, W. M. Star, and B. C. Wilson, "In vivo fluorescence spectroscopy and imaging for oncological applications," *Photochem Photobiol* **68**(5), pp. 603–32, 1998.

24. V. X. Yang, P. J. Muller, P. Herman, and B. C. Wilson, "A multispectral fluorescence imaging system: design and initial clinical tests in intra-operative photofrin-photodynamic therapy of brain tumors," *Lasers Surg Med* **32**(3), pp. 224–32, 2003.

25. V. H. Fingar, W. R. Potter, and B. W. Henderson, "Drug and light dose dependence of photodynamic therapy: a study of tumor cell clonogenicity and histologic changes," *Photochem Photobiol* **45**(5), pp. 643–50, 1987.

26. J. C. van Gemert, M. C. Berenbaum, and G. H. Gijsbers, "Wavelength and light-dose dependence in tumour phototherapy with haematoporphyrin derivative," *Br J Cancer* **52**(1), pp. 43–9, 1985.

27. T. R. Tennant, H. Kim, M. Sokoloff, and C. W. Rinker-Schaeffer, "The Dunning model," *Prostate* **43**(4), pp. 295–302, 2000.

28. B. M. Aveline, T. Hasan, and R. W. Redmond, "The effects of aggregation, protein binding and cellular incorporation on the photophysical properties of benzoporphyrin derivative monoacid ring a (BPDMA)," *J Photochem Photobiol B* **30**(2-3), pp. 161–9, 1995.

29. A. M. Richter, S. Cerruti-Sola, E. D. Sternberg, D. Dolphin, and J. G. Levy, "Biodistribution of tritiated benzoporphyrin derivative (3H-BPD-MA), a new potent photosensitizer, in normal and tumor-bearing mice," *J Photochem Photobiol B* **5**(2), pp. 231–44, 1990.

30. C. C. Lee, B. W. Pogue, J. A. O'Hara, C. M. Wilmot, R. R. Strawbridge, G. C. Burke, and P. J. Hoopes, "Spatial heterogeneity and temporal kinetics of photosensitizer (AlPcS2) concentration in murine tumors RIF-1 and MTG-B," *Photochem Photobiol Sci* **2**(2), pp. 145–50, 2003.

31. C. C. Lee, B. W. Pouge, R. R. Strawbridge, K. L. Moodie, L. R. Bartholomew, G. C. Burke, and P. J. Hoopes, "Comparison of photosensitizer (AIPcS2) quantification techniques: in situ fluorescence microsampling versus tissue chemical extraction," *Photochem Photobiol* **74**(3), pp. 453–60, 2001.

32. C. Sheng, B. W. Pogue, E. Wang, J. E. Hutchins, and P. J. Hoopes, "Assessment of photosensitizer dosimetry and tissue damage assay for photodynamic therapy in advanced-stage tumors," *Photochem Photobiol* **79**(6), pp. 520–5, 2004.

33. E. Demidenko, *Mixed Models: Theory and Applications*, New Jersey, 1st ed. ed., 2004.

34. L. I. Grossweiner, "PDT light dosimetry revisited," *J Photochem Photobiol B* **38**(2-3), pp. 258–68., 1997.

35. L. I. Grossweiner, "Optical dosimetry in photodynamic therapy," *Lasers Surg Med* **6**(5), pp. 462–6, 1986.

36. T. M. Busch, S. M. Hahn, S. M. Evans, and C. J. Koch, "Depletion of tumor oxygenation during photodynamic therapy: detection by the hypoxia marker EF3 [2-(2-nitroimidazol-1[h]-yl)-n-(3,3,3- trifluoropropyl)acetamide]," *Cancer Res* **60**(10), pp. 2636–42., 2000.

37. T. H. Foster and L. Gao, "Dosimetry in photodynamic therapy: oxygen and the critical importance of capillary density," *Radiat Res* **130**(3), pp. 379–83., 1992.

38. I. P. Torres Filho, M. Leunig, F. Yuan, M. Intaglietta, and R. K. Jain, "Noninvasive measurement of microvascular and interstitial oxygen profiles in a human tumor in SCID mice," *Proc Natl Acad Sci U S A* **91**(6), pp. 2081–5, 1994.

39. B. J. Tromberg, A. Orenstein, S. Kimel, S. J. Barker, J. Hyatt, J. S. Nelson, and M. W. Berns, "In vivo tumor oxygen tension measurements for the evaluation of the efficiency of photodynamic therapy," *Photochem Photobiol* **52**(2), pp. 375–85, 1990.

40. J. M. Vanderkooi, G. Maniara, T. J. Green, and D. F. Wilson, "An optical method for measurement of dioxygen concentration based upon quenching of phosphorescence," *J Biol Chem* **262**(12), pp. 5476–82, 1987.

41. S. C. Chang, G. Buonaccorsi, A. MacRobert, and S. G. Bown, "Interstitial and transurethral photodynamic therapy of the canine prostate using meso-tetra-(m-hydroxyphenyl) chlorin," *Int J Cancer* **67**(4), pp. 555–62, 1996.

42. J. S. Dysart, M. S. Patterson, T. J. Farrell, and G. Singh, "Relationship between mTHPC fluorescence photobleaching and cell viability during in vitro photodynamic treatment of DP16 cells," *Photochem Photobiol* **75**(3), pp. 289–95, 2002.

43. M. Niedre, M. S. Patterson, and B. C. Wilson, "Direct near-infrared luminescence detection of singlet oxygen generated by photodynamic therapy in cells in vitro and tissues in vivo," *Photochem Photobiol* **75**(4), pp. 382–91, 2002.

44. M. J. Niedre, C. S. Yu, M. S. Patterson, and B. C. Wilson, "Singlet oxygen luminescence as an in vivo photodynamic therapy dose metric: validation in normal mouse skin with topical amino-levulinic acid," *Br J Cancer* **92**(2), pp. 298–304, 2005.

45. B. Chen, B. W. Pogue, I. A. Goodwin, J. A. O'Hara, C. M. Wilmot, J. E. Hutchins, P. J. Hoopes, and T. Hasan, "Blood flow dynamics after photodynamic therapy with verteporfin in the RIF-1 tumor," *Radiat Res* **160**(4), pp. 452–9, 2003.

46. B. W. Pogue, J. D. Pitts, M. A. Mycek, R. D. Sloboda, C. M. Wilmot, J. F. Brandsema, and J. A. O'Hara, "In vivo NADH fluorescence monitoring as an assay for cellular damage in photodynamic therapy," *Photochem Photobiol* **74**(6), pp. 817–24, 2001.

47. R. K. Jain, "Delivery of molecular and cellular medicine to solid tumors," *Adv Drug Deliv Rev* **46**(1-3), pp. 149–68, 2001.

48. T. Momma, M. R. Hamblin, H. C. Wu, and T. Hasan, "Photodynamic therapy of orthotopic prostate cancer with benzoporphyrin derivative: local control and distant metastasis," *Cancer Res* **58**(23), pp. 5425–31, 1998.

49. G. W. Barendsen, "[experimental data concerning cellular recovery and repopulation of tumors following fractionated irradiation]," *Ned Tijdschr Geneeskd* **113**(48), pp. 2170–1, 1969.

50. Q. Chen, H. Chen, and F. W. Hetzel, "Tumor oxygenation changes post-photodynamic therapy," *Photochem Photobiol* **63**(1), pp. 128–31, 1996.

51. M. Shibata, S. Ichioka, J. Ando, and A. Kamiya, "Microvascular and interstitial pO2 measurements in rat skeletal muscle by phosphorescence quenching," *J Appl Physiol* **91**(1), pp. 321–7, 2001.

52. H. M. Swartz, S. Boyer, P. Gast, J. F. Glockner, H. Hu, K. J. Liu, M. Moussavi, S. W. Norby, N. Vahidi, T. Walczak, and et al., "Measurements of pertinent concentrations of oxygen in vivo," *Magn Reson Med* **20**(2), pp. 333–9, 1991.

53. I. P. Torres Filho and M. Intaglietta, "Microvessel po2 measurements by phosphorescence decay method," *Am J Physiol* **265**(4 Pt 2), pp. H1434–8, 1993.

54. L. Zheng, A. S. Golub, and R. N. Pittman, "Determination of pO2 and its heterogeneity in single capillaries," *Am J Physiol* **271**(1 Pt 2), pp. H365–72, 1996.

55. K. E. Arfors, G. Rutili, and E. Svensjo, "Microvascular transport of macromolecules in normal and inflammatory conditions," *Acta Physiol Scand Suppl* **463**, pp. 93–103, 1979.

56. T. W. Hennigan, R. H. Begent, and T. G. Allen-Mersh, "Histamine, leukotriene C4 and interleukin-2 increase antibody uptake into a human carcinoma xenograft model," *Br J Cancer* **64**(5), pp. 872–4, 1991.

57. H. Maeda, J. Fang, T. Inutsuka, and Y. Kitamoto, "Vascular permeability enhancement in solid tumor: various factors, mechanisms involved and its implications," *Int Immunopharmacol* **3**(3), pp. 319–28, 2003.

58. G. Majno and G. E. Palade, "Studies on inflammation. I. The effect of histamine and serotonin on vascular permeability: an electron microscopic study," *J Biophys Biochem Cytol* **11**, pp. 571–605, 1961.

59. G. Majno, G. E. Palade, and G. I. Schoefl, "Studies on inflammation. II. The site of action of histamine and serotonin along the vascular tree: a topographic study," *J Biophys Biochem Cytol* **11**, pp. 607–26, 1961.

60. D. M. McDonald, "Endothelial gaps and permeability of venules in rat tracheas exposed to inflammatory stimuli," *Am J Physiol* **266**(1 Pt 1), pp. L61–83, 1994.

61. N. Z. Wu and A. L. Baldwin, "Transient venular permeability increase and endothelial gap formation induced by histamine," *Am J Physiol* **262**(4 Pt 2), pp. H1238–47, 1992.